

February 7, 2020

# Capillary forces in the acoustics of patchy-saturated porous media

Yaroslav Tserkovnyak

Lyman Laboratory of Physics, Harvard University, Cambridge, Massachusetts 02138

David Linton Johnson

Schlumberger-Doll Research, Old Quarry Road, Ridgefield, Connecticut 06877

**Abstract.** A linearized theory of the acoustics of porous elastic formations, such as rocks, saturated with two different viscous fluids is generalized to take into account a pressure discontinuity across the fluid boundaries. The latter can arise due to the surface tension of the membrane separating the fluids. We show that the frequency-dependent bulk modulus  $\tilde{K}(\omega)$  for wave lengths longer than the characteristic structural dimensions of the fluid patches has a similar analytic behavior as in the case of a vanishing membrane stiffness and depends on the same parameters of the fluid-distribution topology. The effect of the capillary stiffness can be accounted by renormalizing the coefficients of the leading terms in the low-frequency asymptotic of  $\tilde{K}(\omega)$ .

PACS: 43.20.Jr

## I. Introduction

Using the Biot theory [Biot (1956)] for the acoustics of fluid-saturated porous media as a starting point, [Johnson (2001)] was able to formulate a simple theory for the frequency-dependent bulk modulus,  $\tilde{K}(\omega)$ , of a composite consisting of a homogeneous porous frame heterogeneously saturated with two different viscous Newtonian fluids. It is assumed that saturation occurs in “patches” of 100% saturation of one or the other of the fluids. In the limit when the two fluids are identical, the theory reduces to the low-frequency regime of the Biot theory. [Johnson (2001)] showed that the mismatch of the local properties of the composite across the patch boundaries leads to a dispersion and attenuation mechanism for acoustic waves which is physically

different from that of the Biot theory. In particular, the propagatory modes of the Biot theory, as applied to a fully mono-saturated sample, are predicted to be non-dispersive and non-attenuative in the relevant regime,  $\omega \ll \omega_B$ , where  $\omega_B$  is the Biot crossover frequency. In the case of patchy saturation, on the other hand, the mismatch of the elastic properties at the patch boundaries leads to a redistribution of the fluids between the patches when the system is perturbed. Because of the viscosity, this mechanism governs energy dissipation and, therefore, the attenuation and dispersion of the propagatory modes. There is a cross-over frequency,  $\omega_c$ , below which the pore pressure can equilibrate across the patches and above which it does not.

This mechanism is particularly effective when there is a large contrast between the two fluids as occurs when one of them is a gas. In such a system, which was further studied in [Tserkovnyak and Johnson (2002)] by analyzing measurements of [Cadoret (1993)], the gas saturated patches of the sample may often be approximated as vacuum. The relevant formulae become quite a bit simpler in this case.

While the fluid redistribution across the patch boundaries was of a central importance in the work by [Johnson (2001)], his theory failed to account for the membrane surface tension, which can arise, for example, due to the pinning of the boundary edges inside the pores. The latter will result in the formation of a meniscus when the fluids are pushed between different patches, which in turn leads to a pressure drop between the patches due to the capillary forces. The present paper addresses this phenomenon. It is important to note that various additional capillary effects, such as the fractal nature of the fluid distribution in the pore space, can be important in realistic porous materials but lie outside the scope of this work.

[Johnson (2001)] suggested that the patchy-saturation effect may be a dominant mechanism for the low-frequency ( $\omega \ll \omega_B$ ) attenuation and dispersion in carbonate rocks, but can be dwarfed by microscopic “squirt” mechanisms in materials like sandstones. [Tserkovnyak and Johnson (2002)] indeed showed that the sonic and even ultrasonic measurements [Cadoret (1993); Cadoret *et al.* (1995); Cadoret *et al.* (1998)] on various limestones can be successfully described by the patchy-saturation effect. In particular, we demonstrated there how one can extract information about the characteristic patch sizes and shapes in partially water saturated limestones by measuring the velocity and attenuation of acoustic waves. Extending our theory to take into account the capillary forces is necessary to improve our understanding of the acoustics in patchy-saturated materials.

While the effect of the membrane tension at the boundary is but one of the important effects, investigating it's effects can be a starting point for further studies of the capillary effects in porous media.

The manuscript is structured as follows. In Sec. II we formulate the assumptions and limitations of the theory. Then, in Sec. III we in turn discuss the static, low-frequency, and high-frequency regimes of the theory in the general case of the patchy saturation by two arbitrary fluids. In the subsequent Sec. IV an alternative formulation of the static and low-frequency limits is presented which is simple and physically transparent, albeit only valid for the case when one of the fluids is a gas. We compare our findings with exact numerical calculations in Sec. V for two simple geometries: that of the concentric spheres and the periodic slab geometries. Finally, in Sec. VI a simple theoretical model for  $\tilde{K}(\omega)$  is presented enabling us to connect the low- and high-frequency asymptotics of the theory. Our results are then summarized in Sec. VII. Two somewhat technical discussions, on the analytic structure of  $\tilde{K}(\omega)$  and capillary correction to the high-frequency limit, are given separately from the main text, in Appendices A and B, respectively.

## II. Generalities

As in [Johnson (2001)], we consider a porous rock fully saturated with two different fluids, one having saturation  $S_1$  and the other  $S_2 = 1 - S_1$ . Each point of the sample is thus saturated with one fluid or the other and the local elastic properties of the composite are assumed to be governed by the usual Biot parameters of the rock skeleton and the locally-present fluid. The only exception is the fluid and sample boundaries which deserve a special treatment. While we will talk about various limits of the frequency dependence of the bulk modulus  $\tilde{K}(\omega)$ , the Biot theory is always assumed to be in its low-frequency regime. The Biot crossover frequency

$$\omega_B = \frac{\eta\phi}{k\rho_f\alpha_\infty} \quad (1)$$

[Biot (1956) using the notation of Johnson *et al.* (1994)], defined in terms of the fluid density  $\rho_f$ , the viscosity  $\eta$ , the tortuosity of the pore space  $\alpha_\infty$ , the dc permeability  $k$ , and the porosity  $\phi$ , is thus the upper frequency limit of our theory, i.e., it is assumed that  $\omega \ll \omega_B$ . Biot equations of motion within each fluid patch [Biot (1956)] then

simplify to<sup>1</sup>

$$\nabla \cdot \boldsymbol{\tau} = 0, \quad (2)$$

$$\nabla p_f = \frac{i\omega\phi\eta}{k}(\mathbf{U} - \mathbf{u}), \quad (3)$$

where all quantities vary as  $\mathbf{u}(\mathbf{r})e^{-i\omega t}$ . Here  $p_f$  is the pore pressure,  $\mathbf{U}$  ( $\mathbf{u}$ ) is the displacement of the fluid (solid) phase, and  $\boldsymbol{\tau}$  stands for the total stress due to both (solid and fluid) phases. The pore pressure  $p_f$  and the total stress  $\boldsymbol{\tau}$  are related to the deformation strain in the solid phase,  $\epsilon_{ij} = (1/2)[u_{i,j} + u_{j,i}]$ , and to that in the fluid phase,  $E_{ll} = U_{l,l}$  [Biot (1956)]:

$$\boldsymbol{\tau} = [(P + Q - 2N)\epsilon_{ll} + (R + Q)E_{ll}] \delta_{ij} + 2N\epsilon_{ij}, \quad (4)$$

$$p_f = -\frac{1}{\phi}[Q\epsilon_{ll} + RE_{ll}], \quad (5)$$

where the coefficients  $P$ ,  $Q$ , and  $R$  depend on the bulk moduli of the solid phase,  $K_s$ , of the porous frame,  $K_b$ , and the pore fluid,  $K_f$ , as well as the porosity and the shear modulus of the porous skeleton,  $N$  [see, e.g, Johnson (1986)]. The fast compressional and shear velocities of the Biot theory are non-dispersive and non-attenuative whereas the slow compressional wave is diffusive in the low-frequency limit considered here. Furthermore, we assume that the wave lengths of the fast and shear waves are larger than the characteristic fluid-patch dimension  $L$ , i.e.,  $\omega \ll \omega_x$ , where

$$\omega_x = \frac{2\pi V_{sh}}{L} \quad (6)$$

with  $V_{sh}$  being the (slower) shear-wave velocity. The latter assumption will allow us to define the effective bulk modulus  $\tilde{K}(\omega) \stackrel{\text{def}}{=} -V(P_e/\delta V)$ , where  $(\delta V/V)e^{-i\omega t}$  is the oscillatory fractional volume change in response to an external normal stress,  $\boldsymbol{\tau} \cdot \hat{\mathbf{n}} = -P_e \hat{\mathbf{n}} e^{-i\omega t}$ ,  $\hat{\mathbf{n}}$  being the outward normal of the surface. Finally, the sample is considered to be isotropic and homogeneous, except for the fluid patches.

Due to the capillary forces, the pressure is in general discontinuous across patch boundaries. The relevant

---

<sup>1</sup>These equations do not contain the inertia terms, which is a relevant approximation as the attenuation/dispersion mechanism of our theory is governed by the slow diffusive mode.

boundary condition in the linear-response regime is

$$p_f^{(1)} - p_f^{(2)} = W\phi(\mathbf{U} - \mathbf{u}) \cdot \hat{\mathbf{n}}. \quad (7)$$

Here  $\hat{\mathbf{n}}$  is the outward normal from patch 1 to patch 2,  $p_f^{(i)}$  is the pressure at the boundary on the side of the  $i$ th patch, and  $W$  is a membrane stiffness parameter characterizing the ratio between the pressure drop and the mismatch of the fluid and solid displacements at the boundary. We treat  $W$  as a constant real-valued frequency-independent phenomenological parameter of the theory.  $W$  was measured experimentally for various systems by [Nagy and Blaho (1994)], where the relevance of a simple model for theoretical estimate of this parameter was discussed. See also [Nagy and Nayfeh (1995)]. Form (7) of the membrane stiffness was used by [Nagy (1992)] to analyze his experimental results on surface acoustic modes of fully-saturated porous rocks. In a somewhat different context, boundary condition (7) was used by [Liu and Johnson (1997)] to describe the effect of an elastic mud cake on tube waves in permeable formations. Eq. (7) can be combined with Eq. (3) to generalize the latter to hold at the interfaces as well as inside the patches:

$$\nabla p_f + W\phi[\hat{\mathbf{n}} \cdot (\mathbf{U} - \mathbf{u})]\hat{\mathbf{n}}\delta(R) = \frac{i\omega\phi\eta}{k}(\mathbf{U} - \mathbf{u}), \quad (8)$$

where  $R(\mathbf{r})$  is the shortest distance from a given point  $\mathbf{r}$  to the patch boundary and  $\delta(R)$  is the Dirac's  $\delta$ -function.

In addition, we assume the no net flow condition over the surface of the sample:

$$\int dS[\mathbf{U} - \mathbf{u}] \cdot \hat{\mathbf{n}} = 0, \quad (9)$$

which is valid either for sealed outer boundary or for the periodic boundary conditions. (The integration is taken either over the surface of the sample, for the sealed-pore boundary condition, or over a unit cell, for the periodic boundary conditions.) Eq. (9) can be converted to a volume integral using Gauss' theorem:

$$\langle \epsilon_{ll} \rangle = \langle E_{ll} \rangle. \quad (10)$$

To summarize this section, the present theory supercedes that of [Johnson (2001)] in that the assumption of vanishing capillary forces is now relaxed. The capillarity is accounted by considering the pressure drop across interfaces which is governed by membrane stiffness, see Eq. (7). The theory by [Johnson (2001)] is thus recovered in the limit when  $W \rightarrow 0$ .

### III. High and Low Frequency asymptotics

#### Static regime

In the static limit, it is possible to get an exact closed-form analytic expression for the compressive modulus,  $K_0$ , defined by Eqs. (2)-(7). [Hill (1963)] has developed a well-known exact result for the bulk modulus of a (non-porous) composite in which the shear modulus is everywhere constant, though the bulk modulus varies from point to point. See also [Milton (2001)]. We extend that theory to the present case by looking for solutions of the form

$$\begin{aligned} u_i &= \alpha x_i + \chi_{,i}, \\ U_i &= \alpha x_i + \psi_{,i}. \end{aligned} \quad (11)$$

It is understood that  $\chi$  as well as the normal displacement  $\chi_{,i}n_i$ , are continuous across the patch boundary; similarly for  $\psi$  and  $\psi_{,i}n_i$ . Inasmuch as the first terms in Eqs. (11) are special cases of the second terms, one is free to choose any value for  $\alpha$ , including zero. It is slightly convenient, however, to choose

$$3\alpha = \langle \epsilon_{ll} \rangle \equiv \langle E_{ll} \rangle. \quad (12)$$

Eq. (4) can now be written, within any patch, as

$$\tau_{ij,j} = [(P + Q)\chi_{,jj} + (R + Q)\psi_{,jj}]_i \stackrel{\text{set}}{=} 0. \quad (13)$$

This equation is satisfied if the Laplacians of  $\chi$  and of  $\psi$  are constant within each patch:

$$\chi_{,jj} = \begin{cases} a_1 & \mathbf{r} \in \text{patch 1} \\ a_2 & \mathbf{r} \in \text{patch 2} \end{cases}, \quad (14)$$

$$\psi_{,jj} = \begin{cases} b_1 & \mathbf{r} \in \text{patch 1} \\ b_2 & \mathbf{r} \in \text{patch 2} \end{cases}. \quad (15)$$

The four constants,  $\{a_1, a_2, b_1, b_2\}$ , are determined by various ancillary conditions. First, the volumetric strains within the  $j$ th patch may be written as

$$\begin{aligned} \epsilon_{ll}^{(j)} &= 3\alpha + a_j, \\ E_{ll}^{(j)} &= 3\alpha + b_j. \end{aligned} \quad (16)$$

Therefore, Eq. (12) gives two conditions on the constants:

$$\begin{aligned} S_1 a_1 + S_2 a_2 &= 0, \\ S_1 b_1 + S_2 b_2 &= 0. \end{aligned} \quad (17)$$

Next, there is the condition that the traction,  $\tau \cdot \hat{\mathbf{n}}$ , is continuous across the boundary between patches.

[Hill (1963)] has pointed out an identity satisfied by the discontinuity across the patch boundary of the second derivatives of  $\chi$  which can be rewritten for our purposes as

$$\left[ \chi_{,ij}^{(1)} - \chi_{,ij}^{(2)} \right] n_j = (a_1 - a_2) n_i, \quad (18)$$

where the superscript on  $\chi^{(k)}$  refers to the  $k$ th patch. Therefore, the discontinuity in the traction is

$$\begin{aligned} \left[ \tau_{ij}^{(1)} - \tau_{ij}^{(2)} \right] n_j &= \{[(P_1 + Q_1 - 2N)(3\alpha + a_1) + (R_1 + Q_1)(3\alpha + b_1)] \\ &\quad - [(P_2 + Q_2 - 2N)(3\alpha + a_2) + (R_2 + Q_2)(3\alpha + b_2)] + 2N(a_1 - a_2)\} n_i. \end{aligned} \quad (19)$$

( $P_k, Q_k, R_k$  refer to  $P, Q, R$  evaluated with respect to the saturating fluid in patch  $k$ .) In order for Eq. (19) to vanish across the patch interface, it is necessary that the quantity in brackets,  $\{ \}$ , vanishes:

$$(P_1 + Q_1)(3\alpha + a_1) + (R_1 + Q_1)(3\alpha + b_1) = (P_2 + Q_2)(3\alpha + a_2) + (R_2 + Q_2)(3\alpha + b_2). \quad (20)$$

This, then, is the third condition on  $\{a_1, a_2, b_1, b_2\}$ .

The fourth and final condition follows from Eq. (7). The pore pressure within the  $k$ th patch is given by Eqs. (5) and (16):

$$p_f^{(k)} = -\frac{1}{\phi} [R_k(3\alpha + b_k) + Q_k(3\alpha + a_k)]. \quad (21)$$

We see that the pore pressure is constant within each patch, as required by Eq. (3) in the static limit. The left-hand side of the boundary condition (7) is constant over the interface between the two patches. Consider the case of a finite volume with sealed boundaries. Integrating Eq. (7) over the surface between the two patches, one finds

$$\left[ p_f^{(1)} - p_f^{(2)} \right] A = W\phi \int_A dA (\mathbf{U} - \mathbf{u}) \cdot \hat{\mathbf{n}}, \quad (22)$$

where  $A$  is the area of the interface between the patches. This integration can be extended over the entire bounding surface of fluid 1, say, because there is no flow across the outer boundary:

$$\left[ p_f^{(1)} - p_f^{(2)} \right] A = W\phi \int_{A_1} dA (\mathbf{U} - \mathbf{u}) \cdot \hat{\mathbf{n}}. \quad (23)$$

Now one may use Gauss' theorem:

$$\left[ p_f^{(1)} - p_f^{(2)} \right] A = W\phi \int_{V_1} dV (E_{ll} - \epsilon_{ll}) = W\phi S_1 V \left[ E_{ll}^{(1)} - \epsilon_{ll}^{(1)} \right]. \quad (24)$$

The volumetric strains and the pore pressure can be related to the unknown constants by means of Eqs. (16) and (21), respectively. The result for Eq. (24) is then

$$R_1(3\alpha + b_1) + Q_1(3\alpha + a_1) - [R_2(3\alpha + b_2) + Q_2(3\alpha + a_2)] = \tilde{W}(a_1 - b_1)S_1, \quad (25)$$

where

$$\tilde{W} = W\phi^2 V/A \quad (26)$$

in terms of the sample volume,  $V$ , and the bounding area between the patches,  $A$ . If the derivation is repeated for the case of periodic boundary conditions, Eq. (25) still holds; in that case,  $V$  is the volume of a unit cell and  $A$  is the interface area between the patches within the unit cell. In either case, if the derivation is repeated by closing the surface over fluid 2, instead of fluid 1, the right-hand side of Eq. (25) is replaced by  $-\tilde{W}(a_2 - b_2)S_2$ , which is equivalent via Eqs. (17).

The four linear equations, (17), (20), and (25), can be inverted analytically to get the ratios  $\{a_1, a_2, b_1, b_2\}/\alpha$ ; in practice, this is more easily done numerically. The effective static modulus is simply related to these constants. Following [Hill (1963)], we identify the external pressure,  $P_e$ , with the average compressive stress in the system:

$$P_e = -\frac{1}{3}\langle\tau_{ll}\rangle = -\frac{1}{3} \left[ S_1 \tau_{ll}^{(1)} + S_2 \tau_{ll}^{(2)} \right], \quad (27)$$

where the compressive stress in the  $k$ th patch follows from Eq. (4):

$$\tau_{ll}^{(k)} = 3 \left[ \left( P_k + Q_k - \frac{4}{3}N \right) a_k + (R_k + Q_k)b_k + 3K_{\text{BG}}^{(k)}\alpha \right]. \quad (28)$$

Here  $K_{\text{BG}}^{(k)} = P_k + 2Q_k + R_k - (4/3)N$  is the Biot-Gassmann modulus for the  $k$ th patch. The effective static modulus for the system,  $K_0 = -P_e/\langle\epsilon_{ll}\rangle$ , is thus given by

$$\begin{aligned} K_0 &= \frac{1}{3} \left\{ S_1 \left[ \left( P_1 + Q_1 - \frac{4}{3}N \right) \frac{a_1}{\alpha} + (R_1 + Q_1) \frac{b_1}{\alpha} + 3K_{\text{BG}}^{(1)} \right] \right. \\ &\quad \left. + S_2 \left[ \left( P_2 + Q_2 - \frac{4}{3}N \right) \frac{a_2}{\alpha} + (R_2 + Q_2) \frac{b_2}{\alpha} + 3K_{\text{BG}}^{(2)} \right] \right\}. \end{aligned} \quad (29)$$

Within the context of the model, Eq. (29) is exact. It depends upon the usual Biot parameters, the saturation values, the membrane stiffness,  $W$ , and it also depends upon the surface to volume ratio of the patch interface,  $A/V$ . There are three interesting limiting cases of Eq. (29): (1) If the two fluids have identical bulk moduli, then

$$\lim_{K_f^{(1)} = K_f^{(2)}} K_0 = K_{\text{BG}}^{(1)} = K_{\text{BG}}^{(2)}, \quad (30)$$

independent of the value of the membrane stiffness parameter,  $W$ . When the sample is compressed, the pore pressure rises equally in the two patches with the result that there is no relative flow between fluid and solid. (2) If the membrane stiffness is large enough, then each fluid is locked within its own patch and the static modulus is equal to the Biot-Gassmann-Hill result:

$$\lim_{W \rightarrow \infty} K_0 = K_{\text{BGH}}, \quad (31)$$

where

$$\frac{1}{K_{\text{BGH}} + (4/3)N} = \frac{S_1}{K_{\text{BG}}^{(1)} + (4/3)N} + \frac{S_2}{K_{\text{BG}}^{(2)} + (4/3)N}. \quad (32)$$

(3) If the membrane stiffness is zero, then the static modulus is given by the Biot-Gassmann-Woods result as was proved previously [Johnson (2001)]:

$$\lim_{W \rightarrow 0} K_0 = K_{\text{BGW}}, \quad (33)$$

where  $K_{\text{BGW}} = K_{\text{BG}}(K_f^{\text{eff}})$  and  $K_f^{\text{eff}}$  is an effective fluid modulus given by the Wood's law expression:

$$\frac{1}{K_f^{\text{eff}}} = \frac{S_1}{K_f^{(1)}} + \frac{S_2}{K_f^{(2)}}. \quad (34)$$

In Fig. 1 we show the behavior of  $K_0$  as a function of the lumped quantity  $\tilde{W}$ . The parameter set is that from [Johnson (2001)], reproduced here in Table 1. The sample is saturated with water,  $S_w = 0.7$ , and with air,  $S_a = 0.3$ . If the membrane stiffness is small, then Eq. (33) holds whilst if it is large, Eq. (31) is valid. The crossover occurs when  $\tilde{W}$  is approximately equal to the modulus of the stiffer fluid, water. In Fig. 2 we show the saturation dependence of the static modulus,  $K_0$ , as well as that of  $K_{\text{BGW}}$  and  $K_{\text{BGH}}$ . Even when the membrane-stiffness parameter,  $W$ , is independent of the saturation, the lumped parameter  $\tilde{W}$  will in general have a saturation dependence reflecting the change in the interfacial area. Nonetheless, for this plot,  $\tilde{W}$  is held constant at a value  $\tilde{W} = 1$  GPa.

### Low-frequency limit

Here we wish to find the behavior of  $\tilde{K}(\omega)$  as it approaches  $K_0$ . Using the method developed by [Johnson (2001)], we consider two equivalent expressions for the average energy dissipation per cycle. The macroscopic expression for the dissipation power averaged over one cycle is

$$\bar{P} = \frac{1}{2} \text{Real} \int dS \frac{\partial \mathbf{u}^*}{\partial t} \cdot \boldsymbol{\tau} \cdot \hat{\mathbf{n}} = -\frac{1}{2} \text{Real} \left[ i\omega V \frac{|P_e|^2}{\tilde{K}(\omega)} \right], \quad (35)$$

where the integral is taken over the bounding surface of the sample. The microscopic expression is

$$\bar{P} = -\frac{1}{2} \text{Real} \int dV \phi \left( \frac{\partial \mathbf{U}^*}{\partial t} - \frac{\partial \mathbf{u}^*}{\partial t} \right) \cdot \nabla p_f. \quad (36)$$

In Eq. (36) the integration is taken over the volumes of each patch, specifically excluding the bounding surfaces of the patches;  $\nabla p_f$  has a  $\delta$ -function contribution on the patch surface, see Eq. (8). One may then substitute Eq. (3) into Eq. (36) to arrive at the following microscopic expression for the dissipation:

$$\begin{aligned} \bar{P} &= -\frac{1}{2} \text{Real} \int dV \phi i\omega (\mathbf{U}^* - \mathbf{u}^*) \cdot \left[ \frac{i\omega \phi \eta}{k} (\mathbf{U} - \mathbf{u}) \right] \\ &= \frac{\omega^2 \phi^2}{2k} \int dV \eta(\mathbf{r}) |\mathbf{U}(\mathbf{r}) - \mathbf{u}(\mathbf{r})|^2. \end{aligned} \quad (37)$$

In this expression, the integrand does not contain any  $\delta$ -function contributions. It is immediately clear that, as expected, the low-frequency behavior of  $\bar{P}$  is quadratic in frequency. Therefore, the low-frequency expansion of  $\tilde{K}(\omega)$  is given by

$$\lim_{\omega \rightarrow 0} \tilde{K}(\omega) = K_0 [1 - i\omega T + O(i\omega)^2], \quad (38)$$

where the parameter  $T$  is determined by substituting Eq. (38) into Eq. (35) and equating it to Eq. (37):

$$T = \frac{\phi^2 K_0}{kV|P_e|^2} \int dV \eta(\mathbf{r}) \left[ \mathbf{U}^{(0)}(\mathbf{r}) - \mathbf{u}^{(0)}(\mathbf{r}) \right]^2, \quad (39)$$

which is expressed in terms of the static displacements,  $\mathbf{U}^{(0)}$  and  $\mathbf{u}^{(0)}$ .

We know from Eqs. (11) that the displacements in the static limit are given by the gradient of certain functions. Therefore, we may define an auxiliary function,  $\Phi$ , by

$$\nabla \Phi = -\eta(\mathbf{r}) \frac{\mathbf{U}^{(0)} - \mathbf{u}^{(0)}}{P_e}. \quad (40)$$

Within each patch  $\Phi = \eta[\chi - \psi]/P_e + \text{const.}$  The function  $\Phi$  is continuous across a patch boundary (otherwise there would be a  $\delta$ -function contribution to the displacements); the normal component of the vector  $-\nabla\Phi/\eta(\mathbf{r})$  is also continuous. The function  $\Phi$  satisfies the differential equation

$$\nabla \cdot \left\{ \frac{-1}{\eta(\mathbf{r})} \nabla \Phi \right\} = \frac{E_{ll}^{(0)}(\mathbf{r}) - \epsilon_{ll}^{(0)}(\mathbf{r})}{P_e} \stackrel{\text{def}}{=} g(\mathbf{r}). \quad (41)$$

This equation is analogous to an electrical conductivity problem in which  $\Phi(\mathbf{r})$  plays the role of a potential,  $\eta(\mathbf{r})$  is the local resistivity, and  $g(\mathbf{r})$  is the distributed current source. Electrical neutrality is guaranteed by Eq. (10):  $\int dV g(\mathbf{r}) = 0$ .

In terms of  $\Phi$ , Eq. (39) may be written as

$$T = \frac{\phi^2 K_0}{kV} \int dV \frac{1}{\eta(\mathbf{r})} (\nabla\Phi)^2, \quad (42)$$

which may be integrated by parts:

$$T = \frac{\phi^2 K_0}{kV} \int dV g(\mathbf{r}) \Phi(\mathbf{r}). \quad (43)$$

(The surface term vanishes identically for either the sealed or the periodic boundary condition.) The source function,  $g(\mathbf{r})$ , is constant within each patch but in general is discontinuous across the patch interfaces. From Eqs. (11), (14), and (16) one has

$$g(\mathbf{r}) = \begin{cases} (b_1 - a_1)/P_e & \mathbf{r} \in \text{patch 1} \\ (b_2 - a_2)/P_e & \mathbf{r} \in \text{patch 2} \end{cases}. \quad (44)$$

Thus, the determination of the parameter  $T$  which governs the low-frequency approach to the static limit, Eq. (38), requires solving the differential equation (41) in which the piecewise constant sources, Eq. (44), are known by virtue of the solution for the static regime. This situation is only slightly different from that encountered when the surface-membrane effect is ignored altogether [Johnson (2001)].

### High-frequency limit

Here we consider frequencies that are high in the sense that the pore pressure does not have time to equilibrate from patch to patch but we are still in the regime where  $\omega \ll \omega_B$  and  $\omega \ll \omega_x$ . In this high frequency limit,  $\omega \rightarrow \infty$ , the fluids within each patch are locked with the solid frame,  $\epsilon_{ll} = E_{ll}$ . This conclusion is

independent of the interface-stiffness parameter,  $W$ . We have a situation which satisfies the assumptions of [Hill (1963)]; the shear modulus is a global constant and the bulk modulus is constant within each patch. Hence,

$$K_\infty \stackrel{\text{def}}{=} \lim_{\omega \rightarrow \infty} \tilde{K}(\omega) = K_{\text{BGH}} \quad (45)$$

for any value of  $W$ , where  $K_{\text{BGH}}$  is given by Eq. (32). Recall that we found the same result for the static compressive modulus,  $K_0$ , when the patch boundary is locked by the large capillary tension,  $W \rightarrow \infty$ , see Eq. (31).

For a large but finite frequency, the correction to  $K_\infty$  is provided by the diffusive modes at the patch boundary [Johnson (2001)]. In terms of a local coordinate  $x$  normal to the interface, the pore pressure near the boundary,  $x = 0$ , is given by

$$p_f = \begin{cases} p_{f1} + A_1 e^{-iq_1 x}, & x < 0 \text{ (patch 1)} \\ p_{f2} + A_2 e^{iq_2 x}, & x > 0 \text{ (patch 2)} \end{cases} \quad (46)$$

Here  $p_{fk}$  is the pore pressure inside the  $k$ th patch in the limit of infinite frequency and

$$q_k = \sqrt{i\omega/D_k} \quad (47)$$

is the slow-mode wave vector in terms of the diffusion coefficient  $D_k$ ; see Appendix A. In the case of a finite membrane stiffness,  $p_f(\mathbf{r})$  is in general discontinuous across the patch boundary. We can, nevertheless, show (see Appendix A) that the pore pressure discontinuity  $\delta p_f \stackrel{\text{def}}{=} |p_f^{(1)} - p_f^{(2)}| = O(\omega^{-1/2}) \ll \Delta p_f \stackrel{\text{def}}{=} |p_{f1} - p_{f2}| = O(\omega^0)$ , for large frequencies, and thus the leading correction to  $K_\infty$  can be found by setting  $\delta p_f = 0$ , i.e., assuming continuity of the pressure (46). Requiring, in addition, continuity of the fluid flux, we can then find coefficients  $A_{1,2}$  in Eq. (46) and reproduce the result of [Johnson (2001)]:

$$\lim_{\omega \rightarrow \infty} \tilde{K}(\omega) = K_{\text{BGH}} \left[ 1 - (i\omega)^{-1/2} G + \dots \right], \quad (48)$$

where

$$G = \frac{k K_{\text{BGH}}}{\eta_1 \sqrt{D_1} + \eta_2 \sqrt{D_2}} \left( \frac{\Delta p_f}{P_e} \right)^2 \frac{A}{V} \quad (49)$$

in terms of the would-be drop in the pore pressure,  $\Delta p_f$ , relative to the applied external stress,  $P_e$ :

$$\frac{\Delta p_f}{P_e} = \frac{(R_2 + Q_2)[K_1 + (4/3)N] - (R_1 + Q_1)[K_2 + (4/3)N]}{\phi S_1 K_1 [K_2 + (4/3)N] + \phi S_2 K_2 [K_1 + (4/3)N]}. \quad (50)$$

Notice that the membrane-stiffness parameter does not enter any of Eqs. (48-50), so that the capillary forces not only have vanishing contribution to the high-frequency compressive modulus (45) but also to the leading correction to it, Eq. (48).

## IV. Liquid and vacuum

In the preceding section we have seen that whereas the two terms in the high frequency limit, Eqs. (48), are identical to those derived earlier when  $W = 0$ , the two terms which describe the low frequency limit, Eqs. (38), are now considerably more complicated. The prescription for finding the static bulk modulus,  $K_0$  [Eq. (29)], and the coefficient of the leading low-frequency correction,  $T$  [Eq. (43)], follows from the solution of the system of equations for parameters  $\{a_1, a_2, b_1, b_2\}$ ; no simple analytic form is deduced and no transparent physical interpretation is readily available. We therefore offer an alternative derivation, which is both simple and physically appealing, albeit valid only for the case when one of the two fluids is a gas taken here to be the vacuum, and the other is a liquid whose properties are similar to water or oil. (A gas at STP is four orders of magnitude more compressible than water or oil and so the approximation is a good one except for gas saturations less than  $10^{-4}$ .)

As in Sec. III, the starting point is Hill's theory [Hill (1963)]: If we denote the bulk modulus of the patch saturated with the liquid by  $K'$ , then the static modulus of the composite is given by

$$\frac{1}{K_0 + (4/3)N} = \frac{S}{K' + (4/3)N} + \frac{1 - S}{K_b + (4/3)N}, \quad (51)$$

where  $S$  is the fluid saturation and  $K_b$  is the bulk modulus of the dry frame, as before.  $K'$  can be found by extending the Biot theory: Since the liquid does not bear any shear stresses, the static compressive modulus of the liquid-saturated patch must be given by the Biot-Gassmann formula,

$$K' = K_{\text{BG}}(K'_f) , \quad (52)$$

for some effective fluid bulk modulus,  $K'_f$ . This effective modulus characterizes the “effort of squeezing” the liquid out of the pore space. In particular, two limiting cases are obvious. (1)  $K'_f$  vanishes with the membrane

stiffness:

$$\lim_{W \rightarrow 0} K'_f = 0 \quad (53)$$

and (2) It reduces to the bare fluid modulus for infinitely large stiffness parameter:

$$\lim_{W \rightarrow \infty} K'_f = K_f. \quad (54)$$

If by inducing the pore pressure  $p_f$ , the fluid-filled pore-space volume is reduced by  $\delta V$ , then  $K'_f$  is defined by

$$\frac{1}{K'_f} = \frac{1}{p_f} \frac{\delta V}{\phi SV}. \quad (55)$$

If the fluid volume squeezed out of the pore space into meniscuses formed at the patch surface is  $\delta V'$ , then

$$p_f A = W \delta V', \quad (56)$$

which follows from Eq. (23). Finally, we have

$$\frac{1}{K_f} = \frac{1}{p_f} \frac{\delta V - \delta V'}{\phi SV}. \quad (57)$$

for the bare bulk modulus of the pore fluid. Combining Eqs. (55), (56), and (57) we then arrive at

$$\frac{1}{K'_f} = \frac{1}{K_f} + \frac{A}{W \phi SV}, \quad (58)$$

which satisfies Eqs. (53) and (54) in the two limits given by Eqs. (53) and (54). As a consequence, in the limit  $W \rightarrow 0$ ,  $K' = K_b$  (which is a specific case of a general result holding for arbitrary two fluids:  $K' = K_{\text{BGW}}$ ), and for  $W \rightarrow \infty$ ,  $K' = K_{\text{BGH}}$ . Equations (51), (52), and (58) complete the derivation for the static limit. This result for the static modulus is also plotted in Figures (1) and (2) where it is seen to be identical to that computed from the full formalism.

It is as straightforward to find the parameter  $T$  governing the low-frequency behavior.  $T$  is given by Eq. (43) after solving Eq. (41), when the function  $g(\mathbf{r})$  is known. In the fluid-filled patch, the volumetric strain of the solid can be found using Hill's theory once again [see also Eq. (35) of Johnson (2001)]:

$$\epsilon_{ll} = -\frac{[K_b + (4/3)N]P_e}{K'K_b + (4/3)N[SK' + (1 - S)K_b]}. \quad (59)$$

Using Eq. (5) and

$$p_f A = W\phi SV(E_{ll} - \epsilon_{ll}), \quad (60)$$

provided by Eq. (24), we then obtain

$$E_{ll} - \epsilon_{ll} = -\frac{Q + R}{W\phi^2 SV/A + R} \epsilon_{ll}, \quad (61)$$

which together with Eq. (59) defines the value of  $g$ , Eq. (41), inside the fluid patch:

$$g = \left( \frac{Q + R}{W\phi^2 SV/A + R} \right) \frac{[K_b + (4/3)N]}{K'K_b + (4/3)N[SK' + (1 - S)K_b]}. \quad (62)$$

Here quantities  $Q$  and  $R$  are evaluated using the bare fluid bulk modulus,  $K_f$ . Defining an auxiliary function  $\tilde{\Phi}$  in the space occupied by the fluid patch,  $V_f$ , by

$$\nabla^2 \tilde{\Phi} = -1 \quad \mathbf{r} \in V_f \quad (63)$$

subject to the patch boundary condition  $\tilde{\Phi} \equiv 0$ , we find for the parameter  $T$ , Eq. (43),

$$T = \frac{\eta S \phi^2 K_0 g^2}{k} l_f^2 = \frac{l_f^2}{D_T}, \quad (64)$$

where the coefficient  $D_T$  has the dimensions of a diffusion constant and is given by

$$D_T \stackrel{\text{def}}{=} \frac{k}{\eta S \phi^2 K_0 g^2}. \quad (65)$$

The Poisson size of the fluid patch,  $l_f$ , is defined by

$$l_f^2 \stackrel{\text{def}}{=} \frac{1}{V_f} \int_{V_f} dV \tilde{\Phi}. \quad (66)$$

The sole effect of the membrane stiffness,  $W$ , in this limit, is thus to renormalize the coefficient  $D_T$  from that which held when  $W = 0$ . We have verified numerically that the results derived in this section are identical to those presented in Sec. III when one of the fluids is taken to be a vacuum.

## V. Examples

It is straightforward to repeat the calculations of [Johnson (2001)] for  $\tilde{K}(\omega)$  in which the patchy geometries are either that of periodic slabs or concentric spheres. In the slab geometry, region 1 is a layer of thickness  $L_1$  and

region 2 is a layer of thickness  $L_2$ , periodically repeated. Here  $S_1 = L_1/(L_1 + L_2)$  and  $A/V = 2/(L_1 + L_2)$ .

In the concentric-spheres geometry, region 1 is a sphere of radius  $R_a$  surrounded by region 2 of outer radius  $R_b$ :

$$S_1 = (R_a/R_b)^3 \text{ and } A/V = 3R_a^2/R_b^3.$$

Equations (B.4) and (B.8) of [Johnson (2001)] are still correct as written for the slab and the sphere geometries, respectively. However, the pore pressure is no longer continuous across the patch boundary but it obeys Eq. (7) instead, leading to a slightly different matrix equation to be solved. The results of such numerical calculations are presented in Fig. 3, using the parameter set of Table 1 at a water saturation  $S_w = 0.9$  and assuming a membrane stiffness value of  $W = 30$  GPa/m. The horizontal dashed lines in the left column are  $K_{\text{BGH}}$ ,  $K_0$ , and  $K_{\text{BGW}}$  from high to low, respectively. At low frequencies, we see that the numerically exact results do indeed asymptote to  $K_0$ , as per Eq. (38).  $K_{\text{BGW}}$  has the same value in all three geometries, because the saturation values were chosen to be the same. Similarly for  $K_{\text{BGH}}$ . The values for  $K_0$ , however, are different in the three cases because the surface to volume ratios for the different patch geometries are different. The lumped parameter  $\tilde{W}$  in Eq. (25) has a different value in each case and so, therefore, do the values of  $K_0$ .

As we mentioned earlier, the low-frequency parameter  $T$  is determined by a differential equation (41), which is, in form, identical to that which existed when  $W = 0$  in [Johnson (2001)]. This means that the previously derived results for the slab and the sphere geometries are virtually unchanged. For the sphere, we have from Eq. (40) of [Johnson (2001)]

$$\begin{aligned} T &= \frac{K_0 \phi^2}{30kR_b^3} \{ [3\eta_2 g_2^2 + 5(\eta_1 - \eta_2)g_1 g_2 - 3\eta_1 g_1^2] R_a^5 \\ &\quad - 15\eta_2 g_2(g_2 - g_1)R_a^3 R_b^2 + 5g_2[3\eta_2 g_2 - (2\eta_2 + \eta_1)g_1]R_a^2 R_b^3 - 3\eta_2 g_2^2 R_b^5 \}. \end{aligned} \quad (67)$$

Similarly, the expression appropriate to the slab geometry is Eq. (41) of [Johnson (2001)]:

$$T = -\frac{K_0 \phi^2}{6k(L_1 + L_2)} \{ \eta_1 g_1^2 L_1^3 + 3\eta_1 g_1 g_2 L_1^2 L_2 + 3\eta_2 g_1 g_2 L_1 L_2^2 + \eta_2 g_2^2 L_2^3 \}. \quad (68)$$

Of course, the correct value for the static modulus,  $K_0$ , Eq. (29), and the correct values for  $g_j$ , Eq. (44), must be used. Subject to this clarification, the low-frequency attenuation implied by the second term in Eq. (38) is shown as a dotted line; we see that the numerically computed results asymptote correctly in this limit. It was noted in Sec. III that the high-frequency limit for  $\tilde{K}(\omega)$  is unaffected by a nonzero value for  $W$ . This limit is also plotted

as dotted lines in Fig. 3.

## VI. Theoretical model for $\tilde{K}(\omega)$

A key observation by [Johnson (2001)] was that all singularities and branch cuts of the bulk modulus  $\tilde{K}(\omega)$  must lie on the negative imaginary axis, when analytic continuation into the complex plane is performed. This stems from the diffusive nature of the relaxation mechanism. In Appendix B, we show that this conclusion is not spoiled by a non-zero value for the membrane stiffness and we are, therefore, led to suggest that the simple analytical formula proposed earlier [Johnson (2001)] may work as well here in this new context. We wish to have a function which has singularities only on the negative imaginary axis and which has the limiting properties of Eqs. (38) and (48). That is, we propose the following function should work well as compared against exact numerical results:

$$\tilde{K}(\omega) = K_\infty - \frac{K_\infty - K_0}{1 - \zeta \left( 1 - \sqrt{1 - i\omega\tau/\zeta^2} \right)}, \quad (69)$$

where consistency with Eqs. (38) and (48) requires

$$\tau = \left[ \frac{K_\infty - K_0}{K_\infty G} \right]^2 \quad (70)$$

and

$$\zeta = \frac{(K_\infty - K_0)^3}{2K_0 K_\infty^2 T G^2} = \frac{(K_\infty - K_0)}{2K_0} \frac{\tau}{T}. \quad (71)$$

In Eq. (69) the branch cut in the definition of the square root function,  $\sqrt{Z}$ , is taken to be along the negative real  $Z$ -axis.

For the specific cases of the slab and concentric spheres geometries, the parameter  $T$  is computed directly from Eqs. (67), (68) as the case may be.  $G$  is evaluated using Eq. (49). The resulting predictions from Eq. (69) are shown as dashed curves in Fig. (3), where one can see that it does an excellent job of interpolating throughout the entire frequency range.

## VII. Conclusions

In summary, we have extended the theory of [Johnson (2001)] to consider effects of the capillary forces on the acoustics of porous media saturated with two different fluids. Using a well-known expression for the pore-pressure discontinuity across the patch boundary, Eq. (7), we have shown that the finite membrane stiffness,  $W$ , does not affect the analytic structure of the frequency-dependent bulk modulus  $\tilde{K}(\omega)$ . In addition, the high-frequency asymptotic of  $\tilde{K}(\omega)$  does not depend on  $W$ , as long as  $W$  is sufficiently small [see Eqs. (A10), (A11)], so that the high-frequency limit of our theory can be reached at all. The effect of the capillary forces is thus to rescale the static bulk modulus,  $K_0$ , and the low-frequency correction parameter,  $T$ , Eqs. (29) and (43), respectively. Furthermore, there are no new geometrical parameters introduced by the membrane stiffness: For example, when one of the fluids is a gas, the two relevant topological parameters are the sample-volume to patch-surface ratio and the Poisson size of the fluid patch,  $l_f$ , Eq. (66). In the limit  $W \rightarrow 0$ , the theory of [Johnson (2001)] is recovered. In the limit  $W \rightarrow \infty$ ,  $\tilde{K}(\omega) \equiv K_{\text{BGH}}$ , Eq. (32), for all frequencies.

### Acknowledgments.

This work was supported in part by the NSF Grant DMR 99-81283.

## Appendix A: Capillary correction in the high-frequency limit

In this Appendix we show that the pore pressure discontinuity  $\delta p_f$  across the patch boundary, see Eq. (46), scales as  $\omega^{-1/2}$  at high frequencies,  $\omega \rightarrow \infty$ , so that the membrane stiffness does not modify the high-frequency asymptotic. The pressure equilibration, Eq. (46), is provided by the slow longitudinal waves on both sides of the patch boundary. In order to find equations of motion for the slow wave inside either patch, we take divergence of Eqs. (2), (3) and use relations (4), (5):

$$\nabla^2 \left[ (P_k + Q_k) \epsilon_{ll}^{(k)} + (R_k + Q_k) E_{ll}^{(k)} \right] = 0, \quad (\text{A1})$$

$$\nabla^2 \left[ Q_k \epsilon_{ll}^{(k)} + R_k E_{ll}^{(k)} \right] = \frac{i\omega\phi^2\eta_k}{k} \left[ \epsilon_{ll}^{(k)} - E_{ll}^{(k)} \right]. \quad (\text{A2})$$

Looking for solutions of the form

$$\begin{aligned}\epsilon_{ll}^{(k)} &= c_1^{(k)} \exp^{-i(q_k x + \omega t)} \\ E_{ll}^{(k)} &= c_2^{(k)} \exp^{-i(q_k x + \omega t)}\end{aligned}, \quad (\text{A3})$$

we obtain from Eq. (A1) the ratio of the amplitudes of the solid and fluid phases

$$\frac{c_1^{(k)}}{c_2^{(k)}} = -\frac{R_k + Q_k}{P_k + Q_k} \quad (\text{A4})$$

and then from Eq. (A2) the diffusion coefficient

$$D_k \stackrel{\text{def}}{=} \frac{i\omega}{q_k^2} = \frac{k}{\phi^2 \eta_k} \frac{P_k R_k - Q_k^2}{P_k + 2Q_k + R_k}. \quad (\text{A5})$$

The above equations are valid on both sides of the patch boundary. The coefficients of pressure correction  $A_k$ , Eqs. (46), at the interface are then given by

$$A_k = -\frac{1}{\phi} \left[ Q_k c_1^{(k)} + R_k c_2^{(k)} \right] \quad (\text{A6})$$

where we used Eq. (5) for the additional pressure exerted by the slow waves. The pressure drop  $\delta p_f$  across the interface is related to the relative fluid displacement through Eq. (7), and using Eq. (3) we thus obtain

$$\delta p_f = (p_{f1} + A_1) - (p_{f2} + A_2) = -\frac{q_1 k W}{\eta_1 \omega} A_1. \quad (\text{A7})$$

Finally, we require the fluid-flux continuity across the patch boundary:

$$\frac{q_1}{\eta_1} A_1 = -\frac{q_2}{\eta_2} A_2. \quad (\text{A8})$$

Eqs. (A4), (A6-A8) now constitute a linear system of 6 equations with six unknowns:  $c_1^{(k)}$ ,  $c_2^{(k)}$ , and  $A_k$ . The resulting expression for  $\delta p_f$ , Eq. (A7), simplifies considerably if one patch is filled with a vacuum. In this case, the pressure discontinuity at the fluid boundary, relative to the difference in pore pressure relatively far from the interface is given by

$$\frac{\delta p_f}{\Delta p_f} = \frac{1}{1 + \eta \omega / W k q} = \frac{1}{1 + \sqrt{\omega / i \omega_W}}, \quad (\text{A9})$$

where the crossover frequency

$$\omega_W \stackrel{\text{def}}{=} \frac{W^2 k^2}{\eta^2 D} \quad (\text{A10})$$

is defined in terms of quantities corresponding to the fluid patch. When  $\omega \gg \omega_W$ ,  $\delta p_f \propto \omega^{-1/2}$  and the pressure drop across the interface,  $\delta p_f$ , is negligible in comparison with the pressure difference inside the patches,  $\Delta p_f$ , Eq. (50).

For consistency of our theory, we require that this limit can be reached while we are still in the low-frequency regime of the Biot theory and the propagatory modes have wave lengths longer than the typical patch dimensions, i.e., we need

$$\omega_W \ll (\omega_B, \omega_x). \quad (\text{A11})$$

Eqs. (A10) and (A11) imply that our high-frequency limit is valid only for sufficiently small membrane-stiffness parameter  $W$ . With the parameter set used to generate Figure 3 we have  $\omega_W/(2\pi) = 4.5$  Hz. However, our theory makes no assumption about the value of  $\omega_W$  as compared against the diffusive crossover frequency and, indeed, the theory works quite well even if  $W$  is so large that  $\omega_W$  is greater than the crossover implied by the intersection of the high and low frequency asymptotes.

## Appendix B: Analytic structure of $\tilde{K}(\omega)$

Here we generalize Appendix C of [Johnson (2001)] to take into account the additional term due to the finite membrane stiffness  $W$  in Eq. (8). We want to investigate analytic properties of the real-valued causal response function  $\hat{K}(t)$  in the frequency domain:

$$\tilde{K}(\omega) \stackrel{\text{def}}{=} \int_0^\infty \hat{K}(t) e^{i\omega t} dt. \quad (\text{B1})$$

It is clear that  $\tilde{K}(\omega)$  is analytic everywhere in the upper-half complex  $\omega$ -plane, and we will further show that all the zeros, singularities, and branch cuts lie on the negative imaginary axis.

Below we consider an eigenvalue problem in which all quantities vary as  $\mathbf{u}(\mathbf{r})e^{-i\omega_n t}$ . Assume

$$\int dS \mathbf{u} \cdot \boldsymbol{\tau}^* \cdot \hat{\mathbf{n}} = 0, \quad (\text{B2})$$

as would be in the case of a zero, singularity, or branch cut of  $\tilde{K}(\omega)$ , see [Johnson (2001)]. We can then show using Eq. (2) and the Biot relations between stresses and strains, Eqs. (4) and (5), that  $\int dV p_f \tau_{ll}^*$  is real-valued.

This is true since all these equations are unaffected by the capillary forces, and we thus reproduce Eq. (C5) of [Johnson (2001)]:

$$\int dV p_f \tau_{ll}^* = \int dV \frac{1}{K_b/K_s - 1} \left[ \frac{1}{3} |\tau_{ll}|^2 + \frac{3K_b}{2N} (\mathbf{D}\mathbf{D}^*)_{ll} \right], \quad (\text{B3})$$

where  $D_{ij} = \tau_{ij} - (1/3)\tau_{ll}\delta_{ij}$  is the deviatoric part of the stress tensor. Finally, multiplying Eq. (8) by  $\mathbf{U}^* - \mathbf{u}^*$  and integrating it over the entire volume of the sample, we obtain

$$i\omega_n \int dV \frac{\eta\phi}{k} |\mathbf{U} - \mathbf{u}|^2 = \int dV p_f (\epsilon_{ll}^* - E_{ll}^*) + W\phi \int dV |\hat{\mathbf{n}} \cdot (\mathbf{U} - \mathbf{u})|^2 \delta(R). \quad (\text{B4})$$

As the volumetric strains,  $\epsilon_{ll}$  and  $E_{ll}$ , are given by linear combinations of  $p_f$  and  $\tau_{ll}$  [via inverting Eqs. (4), (5)], the right-hand side of Eq. (B4) is real-valued and, therefore,  $\omega_n$  is pure imaginary. This completes the proof.

## References

Biot, M. A. (1956). "Theory of propagation of elastic waves in a fluid-saturated porous solid. I. Low-frequency range," *J. Acoust. Soc. Am.* **28**, 168-178.

Cadoret, T. (1993). Effet de la saturation eau/gaz sur les propriétés acoustiques des roches; étude aux fréquences sonores et ultrasonores, Ph.D. thesis, 250 pp., L'Université de Paris VII.

Cadoret, T., Marion, D., and Zinszner, B. (1995). "Influence of frequency and fluid distribution on elastic wave velocities in partially saturated limestones," *J. Geophys. Res.* **100**, 9789-9803.

Cadoret, T., Mavko, G., and Zinszner, B. (1998). "Fluid distribution effect on sonic attenuation in partially saturated limestones," *Geophysics* **63**, 154-160.

Hill, R. (1963) "Elastic properties of reinforced solids: Some theoretical principles," *J. Mech. Phys. Solids* **11**, 357-372.

Johnson, D. L. (1986). "Recent developments in the acoustic properties of porous media," in *Frontiers in Physical Acoustics XCIII*, edited by D. Sette, pp. 255-290, North Holland Elsevier, New York.

Johnson, D. L., Plona, T. J., and Kojima, H. (1994) "Probing porous media with first and second sound II. Acoustic properties of water-saturated porous media," *J. Appl. Phys.* **76**, 115-125.

Johnson, D. L. (2001). "Theory of frequency dependent acoustics in patchy-saturated porous media," *J. Acoust. Soc. Am.* **110**, 682-694.

Liu, H.-L. and Johnson, D. L. (1997). "Effects of an elastic membrane on tube waves in permeable formations," *J. Acoust. Soc. Am.* **101**, 3322-3329.

Milton, G., 2001, "The Theory of Composites", (Cambridge University Press, Cambridge).

Nagy, P. B. (1992). "Observation of a new surface mode on a fluid-saturated permeable solid," *Appl. Phys. Lett.* **60**, 2735-2737.

Nagy, P. B. and Blaho, G. (1994). "Experimental measurements of surface stiffness on water-saturated porous solids," *J. Acoust. Soc. Am.* **95**, 828-835.

Nagy, P. B. and Nayfeh, A. H. (1995). "Generalized formula for the surface stiffness of fluid-saturated porous media containing parallel pore channels," *Appl. Phys. Lett.* **67**, 1827-1829.

Tserkovnyak, Y. and Johnson, D. L. (2002). "Can one hear the shape of a saturation patch?" *Geophys. Res. Lett.* **29**, 12.

White, J. E. (1975). "Computed Seismic Speeds and Attenuation in Rocks with Partial Gas Saturation," *Geophysics* **40**, 224-232.

---

$\phi$	0.284
$K_s$	35 GPa
$K_b$	2.637 GPa
$N$	1.740 GPa
$k$	$10^{-13} \text{ m}^2$
$K_f$ (water)	2.25 GPa
$\eta$ (water)	$10^{-3} \text{ Pa s}$
$K_f$ (gas)	$10^5 \text{ Pa}$
$\eta$ (gas)	$10^{-5} \text{ Pa s}$

**Table 1.** Values of input parameters for the calculation of patchy-saturation effects. From [Johnson (2001)].

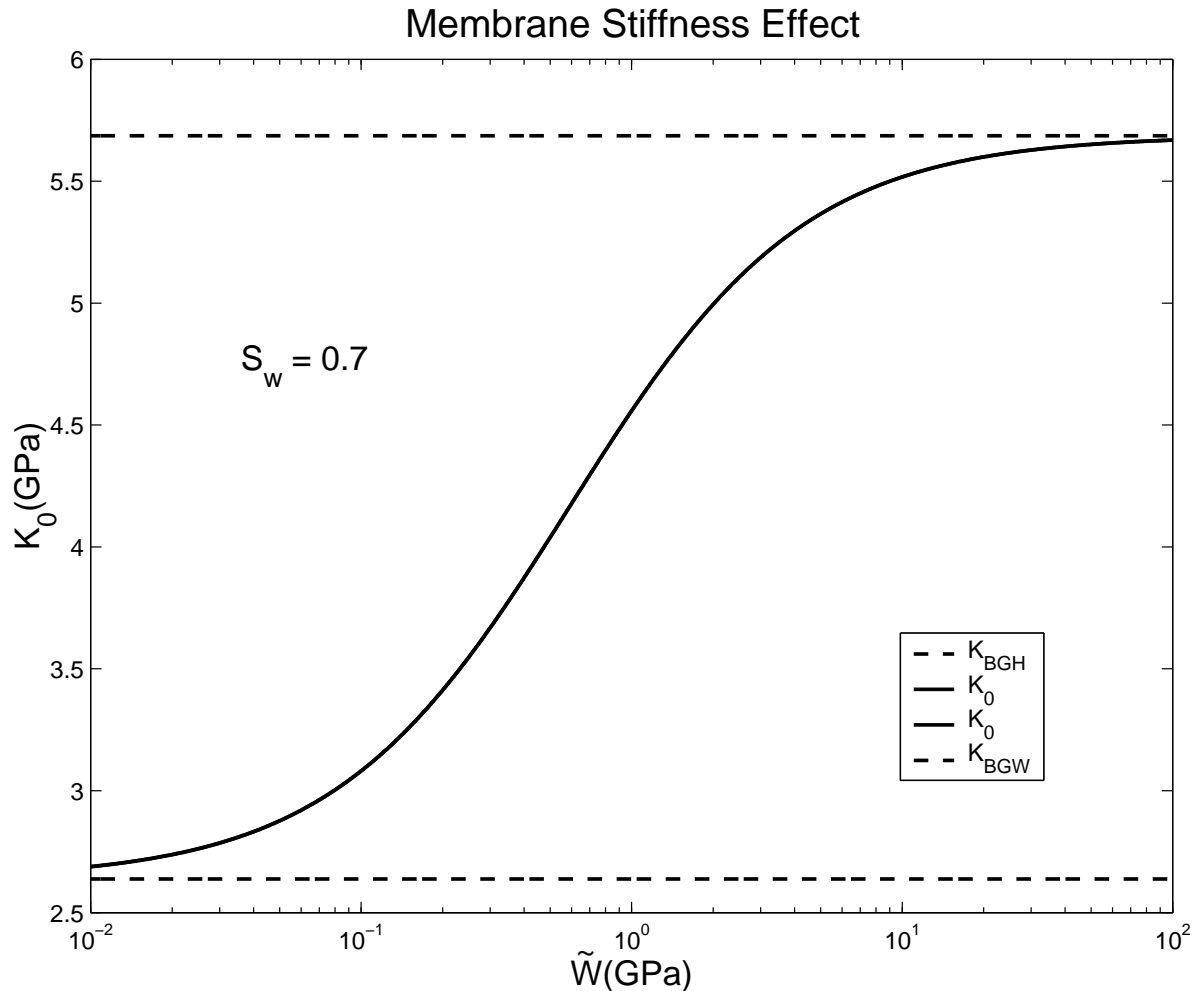


**Figure 1.** Dependence of the static modulus on the lumped quantity  $\tilde{W}$  for a sample saturated with water,  $S_w = 0.7$  and air,  $S_a = 0.3$ . Parameters are listed in Table 1. The two results for the static modulus, Eqs. (29) and (51), are seen to be identical in this case in which one of the fluids is gas.

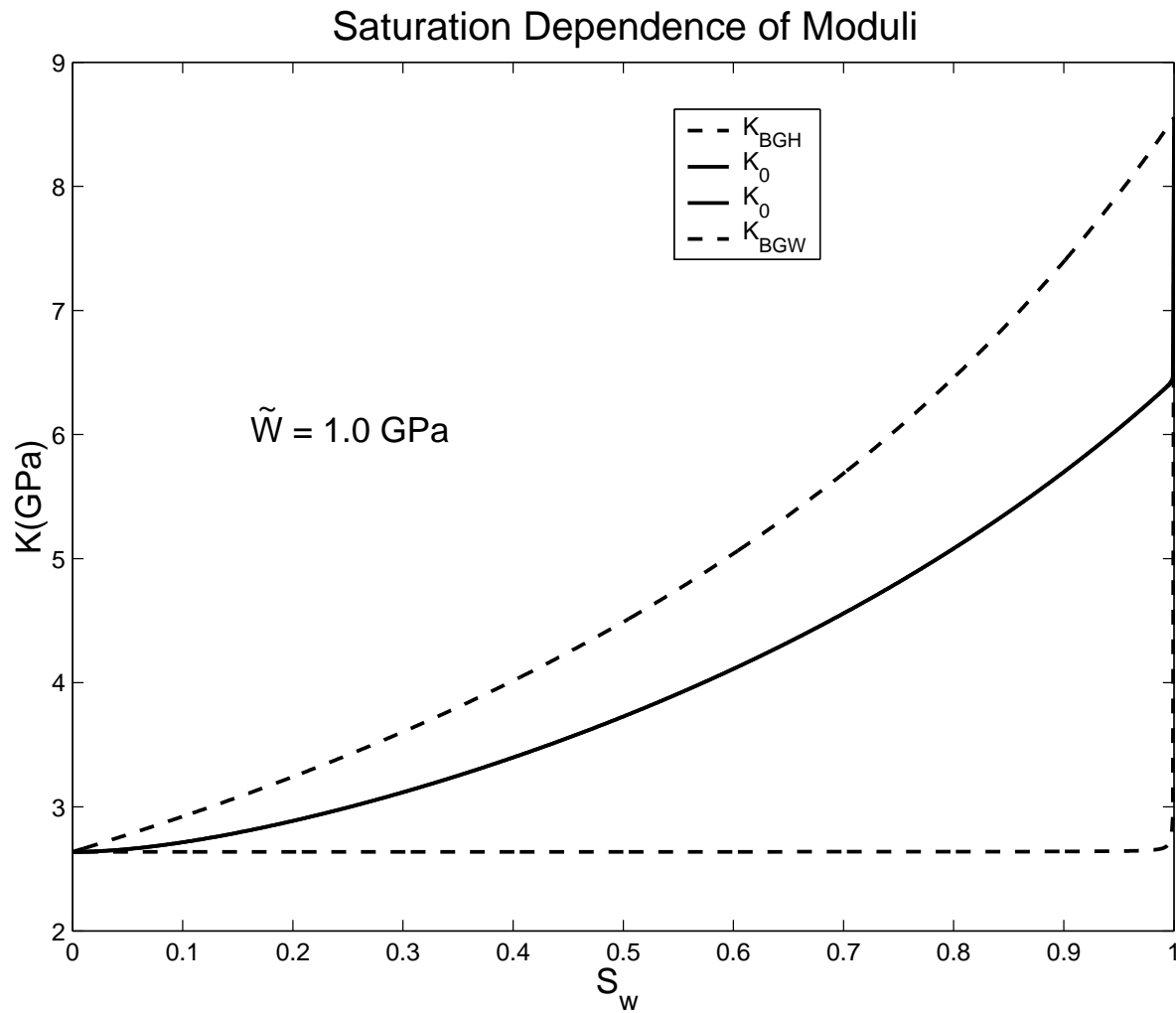


**Figure 2.** The static moduli as a function of the water saturation,  $S_w$ . Parameter set as in Fig. 1. The lumped quantity  $\tilde{W}$  is held constant at a value  $\tilde{W} = 1 \text{ GPa}$ . Again,  $K_0$  is calculated in two different ways.

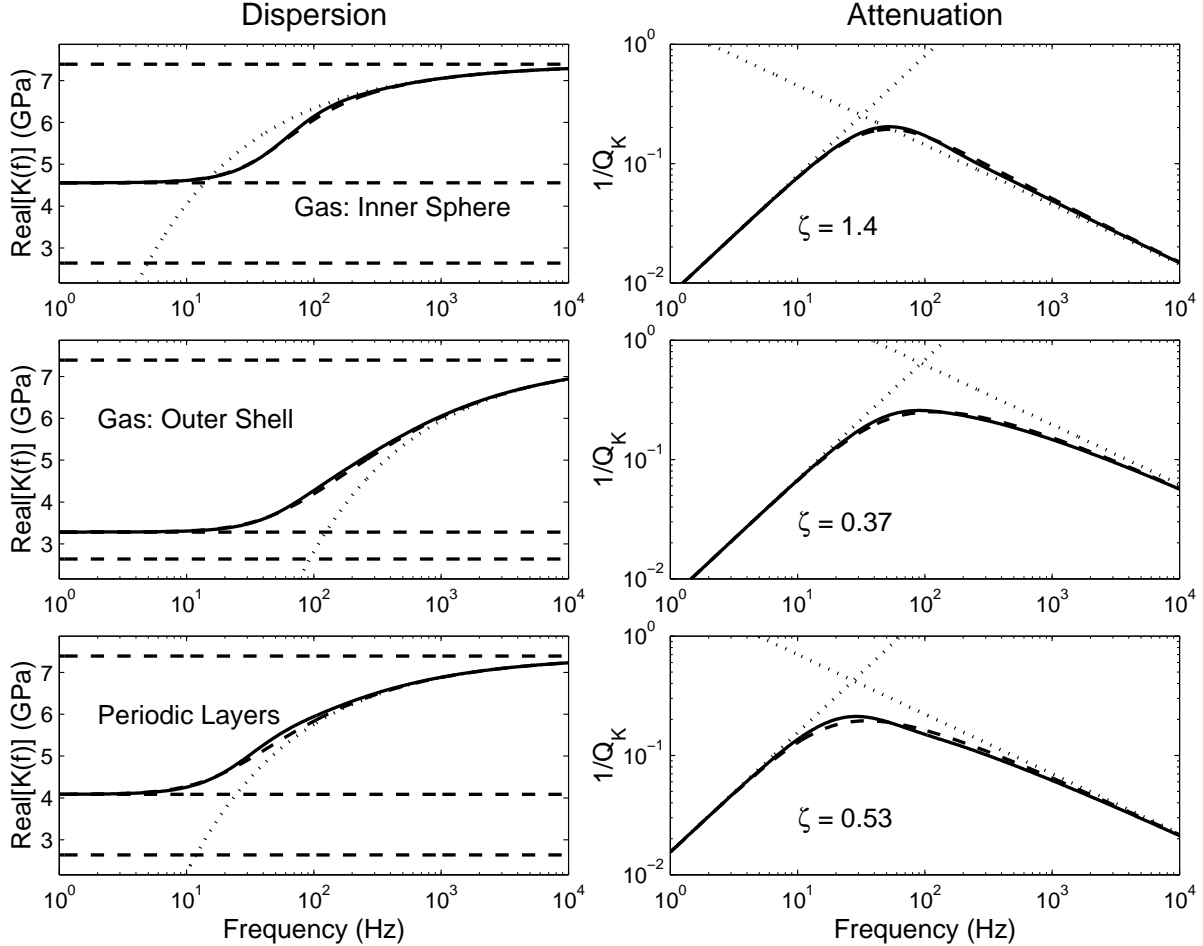


**Figure 3.** Dispersion ( $\text{Real}[\tilde{K}(\omega)]$ ) and attenuation [ $1/Q_K = -\text{Imag}\tilde{K}(\omega)/\text{Real}\tilde{K}(\omega)$ ] due to the patchy-saturation effect for an air/water combination,  $S_a = 10\%$ , in three different situations. Solid lines are numerically exact solutions, dotted lines are the high- and low-frequency limiting expressions, and dashed lines represent the analytic expression. (A) Top Row: The gas is located in an inner sphere,  $R_a = 4.642$  cm, surrounded by a shell of water,  $R_b = 10$  cm. (B) Middle Row: The roles are reversed,  $R_a = 9.655$  cm,  $R_b = 10$  cm. (C) Bottom Row: A periodic slab geometry,  $L_a = 2$  cm,  $L_w = 18$  cm. The other material parameters are listed in Table 1. In all cases, the membrane stiffness is  $W = 30$  GPa/m. The values of  $\zeta$ , Eq. (71), are shown.